Experimental study of coarsening dynamics of the zigzag wall in a nematic liquid crystal with negative dielectric anisotropy

Tomoyuki Nagaya*
Faculty of Education, Okayama University, 3-1-1 Tsushimanaka Okayama, 700-8530, Japan

Jean-Marc Gilli†
Institut Non Linéaire de Nice, UMR 6618 CNRS-UNSA, 1361 Route des Lucioles, 06560 Valbonne, France
(Received 20 September 2001; published 13 May 2002)

When a homeotropically aligned nematic liquid crystal cell is placed above two permanent magnets forming a magnetic quadrupole, a straight splay-bend wall, or a so-called Ising wall, is formed. With a material of positive dielectric anisotropy, it has been shown that the application of an electric field perpendicular to the plates leads to a zigzag instability of the wall, exclusively related to the elastic anisotropy of the liquid crystal. In this case, the coarsening process of the zigzag is very slow, which in turn leads to experimental difficulties concerning its quantitative investigation. If a material of negative dielectric anisotropy is used under an electric field with low voltage and low frequency, two convective rolls appear along the Ising wall due to the charge focusing effect, which is also responsible, at a higher voltage in the homogenous tilted regions, for the appearance of Williams domains electrohydrodynamic instability. If the voltage is higher than a threshold value, the straight Ising wall spontaneously breaks into a zigzag shape and a fast coarsening of the zigzag proceeds, associated with the annihilation of two neighboring vertices. In the present paper, the coarsening dynamics of this system, which can be considered as a one-dimensional Ising situation, are investigated experimentally. At late times, the average width of the zigzag increases logarithmically with time. This finding is consistent with the theory and also with the numerical simulation of a one-dimensional Cahn-Hilliard situation having a conserved order parameter. The scaling analysis of size distribution of the Ising domain, the shape of the power spectrum, and of the correlation function of the Ising order parameter, as well as the number density correlation functions of kinks also confirms that the dynamical scaling law predicted for one-dimensional conservative systems holds for the coarsening process. As supposed from symmetry arguments, it is confirmed that this experiment constitutes a one-dimensional analog of spinodal decomposition.

DOI: 10.1103/PhysRevE.65.051708 PACS number(s): 61.30.Gd, 64.60.Cn, 61.30.Jf

I. INTRODUCTION

For a considerable period in the field of metallurgy, the study of phase ordering dynamics has been conducted in order to understand the experimental characteristics of spinodal decomposition and the nucleation-growth phenomena in binary alloys [1]. In the last two decades, the phase ordering dynamics has been intensively investigated in the field of statistical physics [1,2]. It is well known that the phase ordering dynamics would be classified into several universality classes depending on the spatial dimensionality d, the dimensionality of order parameter n, and the eventual presence of a conservation law. Until the mid-1980s, long term experiments had only focused on a restricted class, where the scalar order parameter $n=1$, in a three-dimensional space, $d=3$. Orihara and Ishibashi [3], in 1986, were the first to use liquid crystals to investigate the phase ordering dynamics. They constructed an ideal two-dimensional system with a nonconserved Ising order parameter, i.e., $d=2$ and $n=1$, in a twisted nematic cell and verified the correlation function in the corresponding system derived theoretically by Ohta, Jasnow, and Kawasaki [4]. Following this pioneering work by Orihara and Ishibashi [3], a number of experimental studies [5–12] that utilize the properties of nematic liquid crystal have been undertaken in various universality classes. This research has stimulated new theoretical studies. It is now well known that liquid crystals are very useful, especially in studies of coarsening dynamics in vector order parameter systems [6–8,10–12], i.e., $n>1$. However, probably due to experimental difficulties, there have not been any detailed experimental studies concerning the one-dimensional system with conserved Ising order parameter.

Recently, Chevallard *et al.* [13] have developed a new experimental system for studying an Ising order parameter system in one-dimensional space. According to their study, a straight splay-bend wall, or the so-called ''Ising wall,'' formed in 4-cyano-4′-pentyl biphenyl (5CB) under a magnetic field, is spontaneously transformed into a zigzagging wall. This spontaneous transformation is brought about by application of a suitable electric field where no electrohydrodynamic convection is induced because the dielectric anisotropy of 5CB is positive. Though the zigzag deformation increases the length of the wall and consequently tends to increase free energy, the twist deformation beside the wall, which was not present before the zigzag transition and replaces the initial exclusive slay-bend deformation, compensates for the increase of wall energy and reduces the total

*Present address: Department of Electric and Electronic Engineering, Faculty of Engineering, Okayama University, 3-1-1 Tsushimanaka Okayama 700-8530, Japan. Electronic address: t_nagaya@cc.okayama-u.ac.jp
†Electronic address: gilli@inln.cnrs.fr

deformation energy of the system. This occurs as the twist deformation is more favorable than the other elastic deformations [14]. The neighboring zigzag vertices attract each other and disappear by coalescence. As a result, the number of zigzags decreases and the average width of the zigzag increases with time. Based only on a consideration of nematic elasticity, Chevallard *et al.* derived the equation of motion for the zigzag wall [13], which is the same as the Cahn-Hillard equation [15]. Since the zigzag wall can be idealized as kink-antikink in one-dimensional space, the coarsening process of the zigzag wall can be regarded as a spinodal decomposition in a one-dimensional system. However, they did not analyze the quantitative features of the coarsening of the zigzag wall owing to experimental difficulties: in particular, the coarsening itself is generally in competition with a global reorientation of the wall that possesses a finite length associated with the limited extension of the sample. Following this study, the present authors have reported that a similar zigzag instability and a similar time evolution of zigzag pattern also takes place in *p*-methoxybenzilidene-*p'*-*n*-butylaniline (MBBA) under a magnetic field by application of a low-frequency electric field, in which a electrohydrodynamic convection is induced by the electric field due to the negative dielectric anisotropy of MBBA [16].

Unlike the case for 5CB, it is very difficult to derive the equation of motion for the zigzag wall in MBBA because not only the anisotropy of the elastic constants, but also the hydrodynamic convection play an important role in the zigzag instability. The hydrodynamics can probably be considered here as a simple amplifier of the elastic anisotropy effect, which strongly accelerates the coarsening process. From a symmetry point of view, the explanation for the presence of a conserved quantity in the coarsening process remains the same in both the experiments. It is derived from the geometrical constraints of the problem: the zigzag process is not associated with a global translation perpendicular to the initial straight wall, and, as explained in detail in the following comments on Fig. 8, it comes from the trivial conservation of the zig and zag projection length, along the initial straight wall. It is consequently very clear from the continuity of the wall and the restriction of the zigzag angle that the time evolution of the zigzag wall can also be considered as one-dimensional spinodal decomposition. It is demonstrated therefore that the equation of motion for the zigzag wall in MBBA is also described by the Cahn-Hilliard equation. Although the mechanisms of the zigzag instabilities in both systems are not exactly the same, they both give the same opportunity to investigate experimentally the spinodal decomposition with conserved order parameter in the one-dimensional space situation. Strictly speaking, it is possible that there is a small discrepancy in the initial distribution of the zigzag wall in both systems because of different zigzag instabilities in both systems. In the present paper, due to the experimental accessibility of the zigzag wall in MBBA, the authors chose to first investigate the coarsening process of the zigzag wall in the case of MBBA from the viewpoint of spinodal decomposition. The experimental data for 5CB will be reported elsewhere.

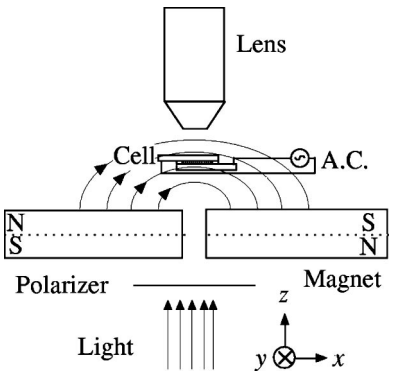

FIG. 1. Experimental setup.

This paper is organized as follows. In the following section, the experimental setup is briefly described. In Sec. III, the experimental results are shown, and then analyzed based on the scaling concept. The last section is devoted to summarizing the present work.

II. EXPERIMENT

A. Setup

The experimental setup is similar to those described in Ref. [17]. The liquid crystal used is MBBA at room temperature. This possesses a sufficiently high magnetic susceptibility and a negative anisotropy for dielectric constants. The elastic constants of MBBA are anisotropic [18]: $K_1=6\times10^{-7}$ dyn, $K_2=4\times10^{-7}$ dyn, $K_3=7.5\times10^{-7}$ dyn at approximately 25 °C. To induce electrohydrodynamic convection, a conductive impurity, tetra-n-butylammonium bromide, was added to the liquid crystal at a concentration of 0.05 wt. %. The liquid crystal was sandwiched between two parallel glass plates coated with transparent electrode. The thickness and the cell size were $d_{\mathrm{gap}}=50$ μm and 2×2 cm^2, respectively. To obtain homeotropic alignment, a surfactant (Nissan Chemical Industries, SUNEVERSE-1211) was coated on the glass plates.

As illustrated in Fig. 1, the sandwiched cell was placed above two permanent Nd-Fe-B magnets, which produce a slightly inhomogeneous magnetic field inside the cell. The dimension of the magnet was $51\times51\times12$ mm^3. Here, only one polarizer was inserted under the magnets. Although the strength of the magnetic field was controlled by varying the distance between the cell and the magnets, the distance was fixed at 6 mm for the present experiment. The value of the horizontal component of the magnetic field at the position of the Ising wall was approximately 315 mT. Due to the inhomogeneity of the magnetic field, there was an equilibrium position for the straight Ising wall within the microscope observation field. If the wall was removed from its equilibrium position, the magnetic field exerted a restoring force on the wall. Without the electric field, it took approximately 1 h for the wall to return to the equilibrium position if the wall deviated from its equilibrium position by 50 μm. Since the vertices of the zigzag deviate from their initial equilibrium positions by a maximum of approximately 50 μm at the end of observations under the electric field, i.e., $t=2048$ s, the

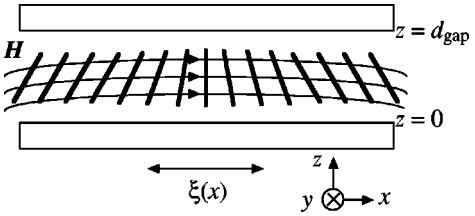

FIG. 2. Schematic illustration of molecular orientations around the Ising wall. The thickness wall is estimated as $\xi(x)=\sqrt{k/\chi}/H$.

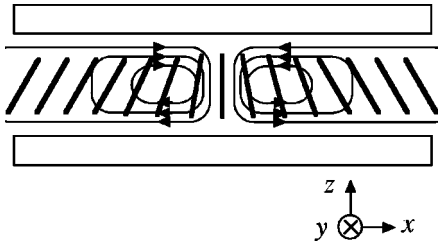

FIG. 3. Schematic illustration of the stream of two convective rolls around the Ising wall.

influence of the restoring force on the dynamics of the wall is considered to be small during the observation time. For simplicity therefore, the restoring force and the inhomogeneity of magnetic field are ignored in the present paper.

The applied ac electric field was supplied by a synthesizer (NF Electric Instruments, WF 1944) and an amplifier (NF Electric, Instruments HSA 4011). To obtain the zigzag regime, the applied voltage was fixed as 8 V for the present experiment. The frequency of the ac field was also fixed as 20 Hz. A charge-coupled device camera (SONY XC-8500CE) of CCIR standard mounted on a microscope (Olympus, BX-60) sent the image signal to a video capture board (Scion Corporation, LG-3). A sequence of images consisting of 12 snapshots with an exponential time step based on 2 s were stored in a personal computer (Apple, PowerMacintosh 9600), where the images were digitized into 256 gray levels and 760×512 pixels. Image analyses described in a following subsection were undertaken using NIH-Image (National Institute of Health in USA NIH-Image) with originally developed subprograms. The statistical quantities discussed in the present paper are evaluated from ten runs of the same experiment.

III. RESULTS AND DISCUSSIONS

A. Zigzag instability

As illustrated in Fig. 2, the splay-bend wall, i.e., the Ising wall, is formed under an inhomogeneous magnetic field where the Ising wall is straight along the y axis and perpendicular to the magnetic flux. The half width of the Ising wall is estimated as $\xi(x)=\sqrt{k/\chi}/H$, where k, χ, and H are the averages of elastic constants for splay and bend deformations, the magnetic susceptibility, and the magnetic field, respectively [14]. When a low voltage is applied to the cell, two wide convective rolls are induced along the Ising wall. The axes of rolls are parallel to the Ising wall. By observing trajectories of dust particles in the cell, it is found that there is a downstream only on the Ising wall as illustrated in Fig. 3. It should be recalled that under a homogeneous magnetic field there is a threshold voltage for electrohydrodynamic instability. The existence of the threshold voltage suggests that it takes a certain amount of energy to break the mirror symmetry at the center plane $z=d_{\mathrm{gap}}/2$ of the cell by inducing the convection. In the present system, however, the convection appears under voltage as low as 0.7 V. From the viewpoint of symmetry, the authors consider that the convection may exist under an infinitesimal electric field because the mirror symmetry is initially broken inside the splay-bend wall formed before applying the electric field. However, they were unable to confirm experimentally whether the threshold voltage that induced the convection exists or not, since the very faint flow under the weak electric field would not be able to drag dust particles.

When the voltage is higher than the threshold voltage for zigzag formation, $V_{\mathrm{th}}=6.9$ V, a sinusoidal undulation appears in the wall and it develops into the zigzag undulation as time progresses. The typical time evolution of the wall after the application of an electric field is shown in Fig. 4. After $t\sim16$ s, the undulation of the wall becomes visible and transforms into a zigzag. In late times, after $t\sim64$ s, the coarsening of the zigzag wall proceeds. In this coarsening process, two adjacent vertices attract each other and the mutual distance between them decreases with time, demonstrating therefore, the presence of an attractive interaction between neighboring vertices. Finally, the two adjacent vertices of opposite directions annihilate each other.

The zigzag instability in the present system does not occur under the high-frequency electric field for which there is no electrohydrodynamic convection. Moreover, if very pure MBBA is used, both the electrohydrodynamic convection and the zigzag instability cannot be observed. It is therefore expected that the zigzag instability displayed in this experiment, using a negative dielectric anisotropy nematic liquid

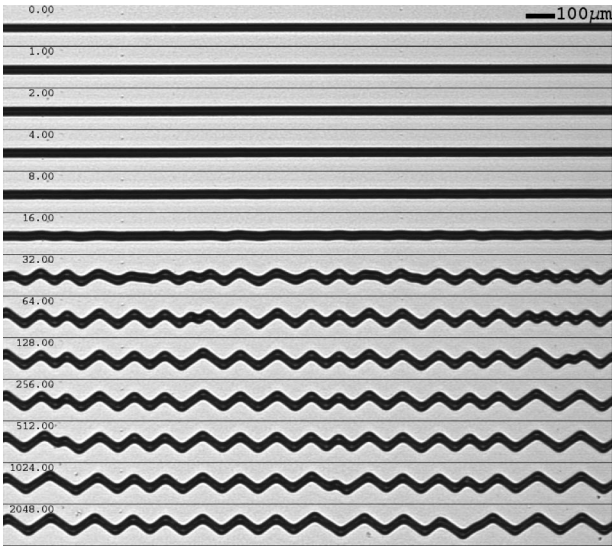

FIG. 4. Time evolution of the wall. The horizontal and vertical directions in the photographs correspond to the y and x axes, respectively. The magnetic field is parallel to the vertical direction.

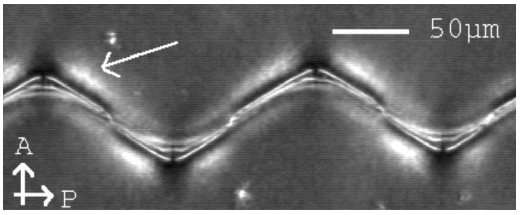

FIG. 5. Observation of zigzag wall under the crossed polarizers. There is a twist deformation component in the bright area indicated by the arrow.

crystal, is strongly related to the electrohydrodynamic convection. It is known that in a nematic liquid crystal with positive dielectric anisotropy, the zigzag instability is driven by the elastic anisotropy of splay, twist, and bend deformations [13]. It is natural to assume that the anisotropy of elastic constants also plays an important role in the zigzag instability in the present system. This conjecture is confirmed by an observation under the crossed polarizers. It is clearly shown in Fig. 5 that there are bright regions next to the wall vertices in which the twist deformation exists (for example, see the arrow in Fig. 5). The slope and width of the zigzag depend on the voltage, the frequency of the applied electric field, and the magnetic field. In the present paper, however, such applied field dependencies and the mechanism of zigzag instability are not dealt with. These will be reported elsewhere.

B. Analysis

A smoothing operation is initially undertaken to remove any short wavelength noise from the image and a binary image, i.e., a black and white image, is created by setting a suitable intensity threshold. Next, the center of zigzagging line is extracted. A least square fitting for each straight part of the zigzagging line is then applied and a position and a local slope, $\Psi(y,t)$, of zigzag are estimated.

The time evolution of the mean value of $|\Psi(y,t)|$ is indicated in Fig. 6. It should be noted that the slope of the zigzag saturates to a fixed value at $t\sim 64$ and does not change at subsequent times. In order to discuss the spinodal decomposition in a one-dimensional Ising system, an Ising order parameter $\Lambda(y,t)$ defined as

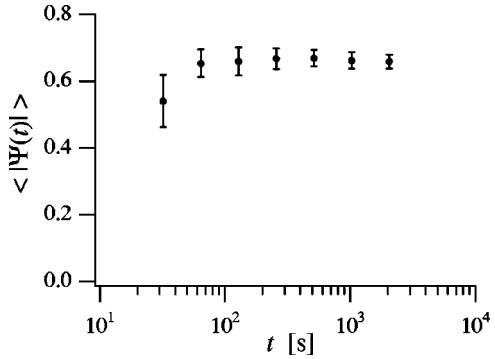

FIG. 6. Time evolution of the average slope of zigzag.

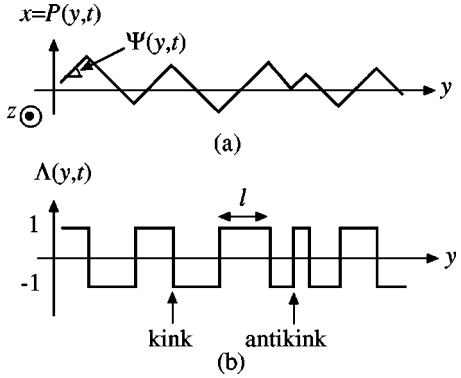

FIG. 7. Relation between (a) the zigzaging pattern and (b) the order parameter $\Lambda(y,t)$.

$$\Lambda(y,t)=\begin{cases}1 & \text{if } \Psi(y,t)>0,\\ -1 & \text{if } \Psi(y,t)<0,\end{cases} \tag{1}$$

is introduced. As illustrated in Figs. 7(a) and 7(b), the order parameter vanishes only on the vertices considered as kinks. Hereafter a kink that corresponds to the upward vertex is defined as a positive kink and a kink that corresponds to the downward vertex is defined as a negative kink.

Here let us focus on the annihilation process of neighboring vertices that are located very closely together, as shown in Figs. 8(a) and 8(b), and the conservation law of the order parameter. Suppose that the lengths of the positive and the negative slopes are denoted as a_i and b_i, respectively, as shown in Fig. 8(b). Since the vertices indicated by the arrows in Fig. 8(a) hardly move during the annihilation process, a_1, a_4, and b_1 do not change. On the other hand, a_2, a_3, b_2, and b_3 change. It can be easily understood that both sums a_2+a_3 and b_2+b_3 are conserved in this annihilation process since the zigzag line cannot move freely due to the strong restriction of the slopes. In the coarsening process of the zigzag wall therefore, the total lengths of the positive and negative slopes do not change, i.e., $\Sigma_i a_i(t)=\text{const.}$ and $\Sigma_i b_i(t)=\text{const.}$ It is obvious that their projection lengths on the y axis are also conserved. Consequently, the conservation law that characterizes the dynamics is expressed as

$$M=\int \Lambda(y,t)dy, \tag{2}$$

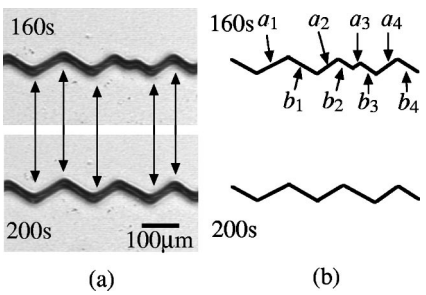

FIG. 8. Snapshots of the annihilation of vertices. (a) Upper and lower parts correspond to 160 s and 200 s after application of the electric field respectively. (b) The center of zigzag traced from (a).

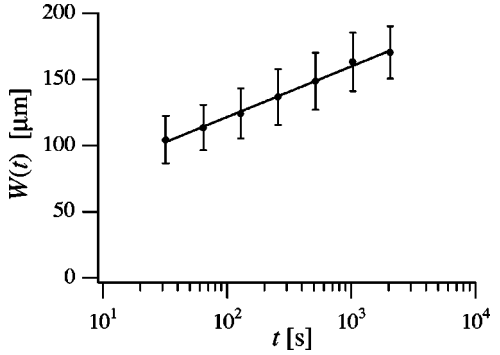

FIG. 9. Time evolution of the average width of zigzag.

where M is a time independent constant close to zero in the present experiment [13]. Strictly speaking, however, this conservation law does not hold for the long time limit. At this point there are only a few zigzags and the ends of the zigzag at the boundaries of cell can move if the magnetic field is homogeneous in the cell. However, the present system can be adequately regarded as a conserved order parameter system during the observation as the width of zigzag at $t=2048$ s is less than one hundredth of the cell size.

The coarsening dynamics of the zigzag wall at late times where $t>64$ s will now be considered. The time dependence of the width of the zigzag $W(t)$, is defined by the average distance between the upward or downward vertices, and is shown in Fig. 9. It should be noted that the average width of the zigzag increases logarithmically with time, $W(t)\sim\ln(t)$. This is a characteristic feature of the coarsening dynamics of kinks in a one-dimensional system with the conserved order parameter predicted by the theory [19] and the numerical simulation [20]. In order to analyze the structure of kinks, a distribution function of the domain size is introduced, defined by

$$g(l,t)=\frac{1}{N(t)}\sum_{i=1}^{N(t)}\delta(y_{i+1}(t)-y_i(t)-l), \tag{3}$$

where $N(t)$ and $y_i(t)$ denote the total number of kinks in the observed area and the position of ith kink at time t, respectively [21]. The probability that a domain can take a size comprising the interval $(l,l+dl)$ becomes $g(l,t)dl$. As shown in Fig. 10, there is a peak for a length value $l_p(t)$,

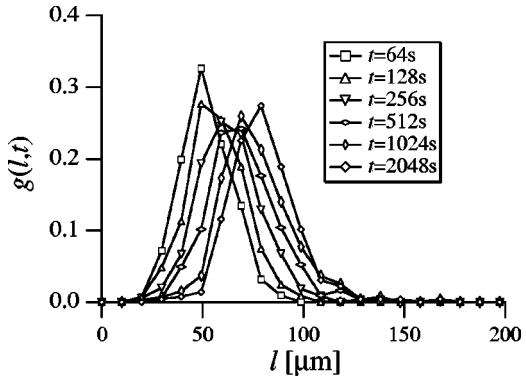

FIG. 10. Distribution function for domain size.

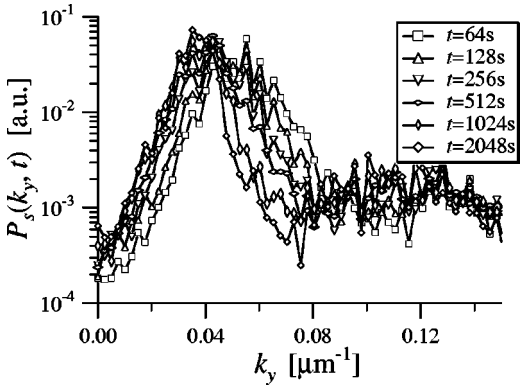

FIG. 11. Power spectrum of the order parameter $\Lambda(y,t)$.

which is almost the same as $W(t)/2$. In the late stage after $t\sim 64$ s, the shapes of $g(l,t)$ at differing times are very similar. The cutoff length $l_c(t)$, which exists in the nonconserved order parameter system [21,22], also exists in the present system, below which $g(l,t)$ is very small and above which $g(l,t)$ shows rapid increase, and $l_c(t)$ moves to larger l with increasing t. This means that domains with sizes smaller than $l_c(t)$ have been annihilated while domain sizes larger than $l_c(t)$ still survive. The shape of $g(l,t)$ is asymmetric, i.e., it is sharp on the lower side of the peak and slightly broad on the upper size. It can be assumed that the short-range interaction between the neighboring vertices is very strong like an exponential attractive force, as supposed in the theory [22] and the simulation [20]. It should be mentioned that the shapes of $g(l,t)$ obtained in the present experiment are not similar to those in the numerical simulation and the theoretical prediction for the nonconserved order parameter system by Kawasaki *et al.* [21,22] where the distribution of domain size has very long tail in the size $l\gg l_p(t)$. In the present system, as shown in Fig. 4, the zigzag is relatively regular in late times, namely, the domains are distributed narrowly, which seems to be a characteristic feature of a conserved order parameter system.

Other important physical quantities allowing for comparison between experiment and theory in addition to $g(l,t)$ are the power spectrum $P_s(k_y,t)$, i.e., structure function, and the spatial correlation function $C(y,t)$ defined by the following equations:

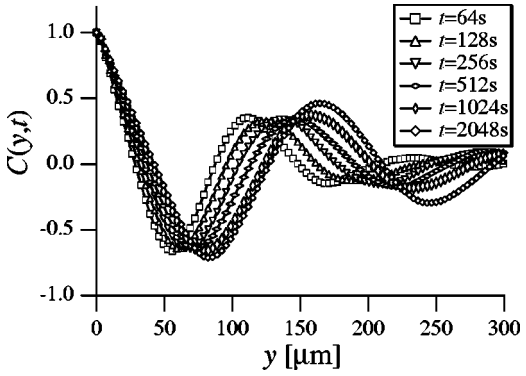

FIG. 12. Autocorrelation function of the order parameter $\Lambda(y,t)$.

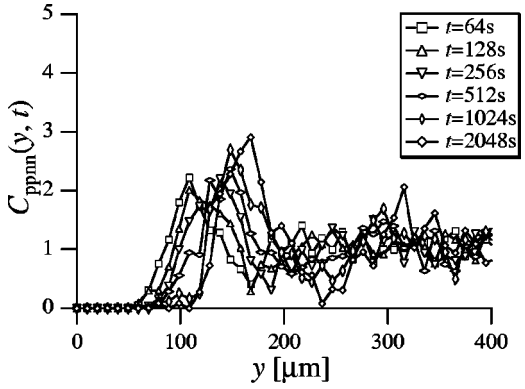

FIG. 13. Number density correlation function of kinks with same sign.

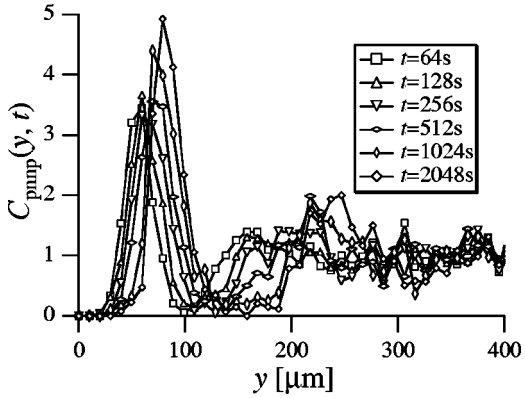

FIG. 14. Number density correlation function of kinks with opposite sign.

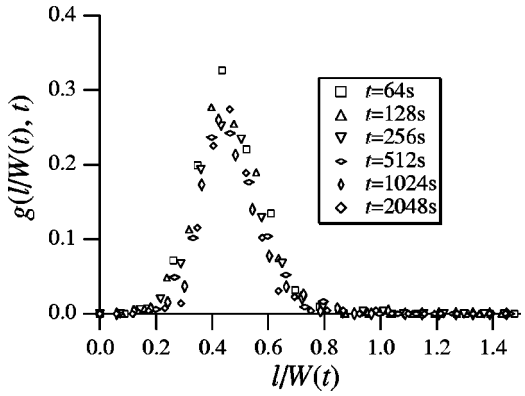

FIG. 15. Scaled size distribution function.

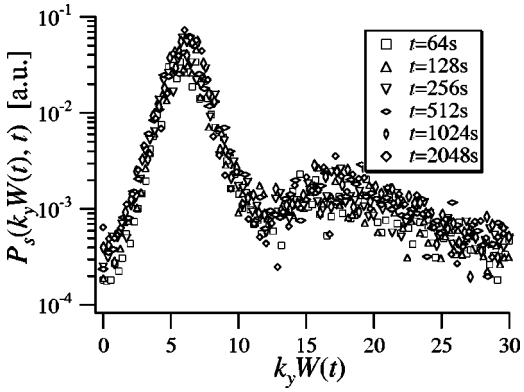

FIG. 16. Scaled power spectrum of the order parameter $\Lambda(y,t)$.

$$P_s(k_y,t)=|\Lambda(k_y,t)|^2, \tag{4}$$

$$C(y,t)=\langle\Lambda(y,t)\Lambda(0,t)\rangle, \tag{5}$$

where $\Lambda(k_y,t)$ is a Fourier coefficient of $\Lambda(y,t)$ and $\langle\cdot\rangle$ denotes spatial average along the y axis. In these calculations, a periodic boundary condition is assumed. The power spectrum and the spatial correlation function are presented in Figs. 11 and 12, respectively. The power spectrum has a characteristic peak at $k_y=2\pi/W(t)$, which corresponds to the wavelength of periodic oscillation in $C(y,t)$. It should be noted from Figs. 11 and 12 that in the late stage both the power spectrum and the correlation function at different times have the same functional form, except for the abscissa scales.

The distribution of positive and negative domains of $\Lambda(y,t)$ in relation to the distribution of the positive and negative kinks is considered next. In the study of phase ordering dynamics, the number density correlation functions for kinks of the same and the opposite signs are also regarded as important physical quantities [6,23]. Suppose $p(y,t)$ and $n(y,t)$ are number densities of positive and negative kinks, denoted by following equations, respectively,

$$p(y,t)=\sum_i \delta(y-y_i^{(p)}(t)), \tag{6}$$

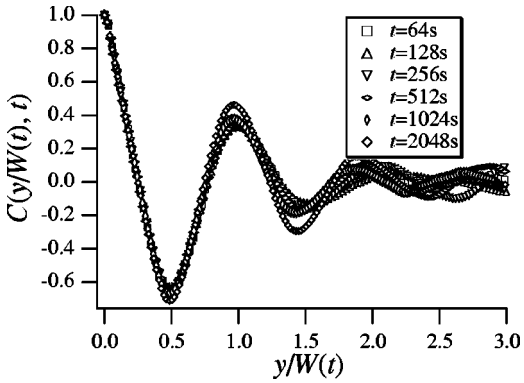

FIG. 17. Scaled autocorrelation function of the order parameter $\Lambda(y,t)$.

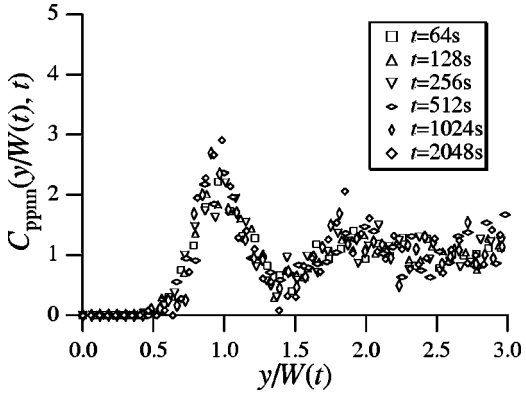

FIG. 18. Scaled number density correlation function of kinks with same sign.

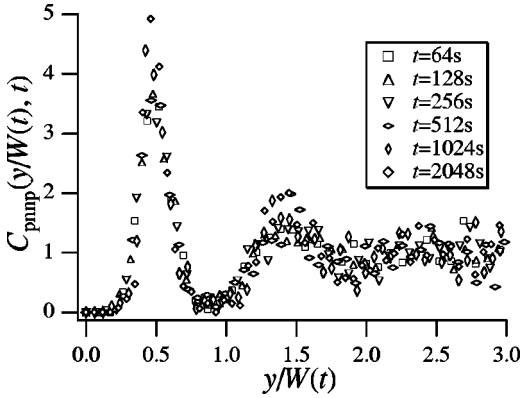

FIG. 19. Scaled number density correlation function of kinks with opposite sign.

$$n(y,t)=\sum_i \delta(y-y_i^{(n)}(t)), \tag{7}$$

where $y_i^{(p)}(t)$ and $y_i^{(n)}(t)$ are the position of ith positive kink and that of ith negative kink, respectively. Then the correlation function of the number density of kinks of the equal sign is defined as [23]

$$C_{ppnn}(y,t)=\frac{\langle p(y,t)p(0,t)+n(y,t)n(0,t)\rangle}{\langle p(0,t)\rangle^2+\langle n(0,t)\rangle^2}. \tag{8}$$

Similarly, that of the opposite sign is defined as

$$C_{pnnp}(y,t)=\frac{\langle p(y,t)n(0,t)+n(y,t)p(0,t)\rangle}{2\langle p(0,t)\rangle\langle n(0,t)\rangle}. \tag{9}$$

If there is no correlation between the kinks, neither number density correlation function depends on y but instead takes unity value. On the other hand, the correlation between the kinks decreases with an increase in their mutual distance and the number density correlation function approaches unity value only at the long distance limit.

The number density correlation function for the kinks having the same sign is shown in Fig. 13. Since there is a kink of opposite sign between the neighboring kinks having the same sign, $C_{ppnn}(y,t)$ vanishes in a distance regime shorter than the average domain size $W(t)/2$. Above $y \sim W(t)/2$, $C_{ppnn}(y,t)$ increases and reaches a maximum value at $y \sim W(t)$. Above the peak, $C_{ppnn}(y,t)$ shows oscillatory convergence to unity where the period of oscillation is equal to $W(t)$. The number density correlation function for the kinks of opposite signs is shown in Fig. 14. It is remarkable that $C_{pnnp}(y,t)$ practically vanishes in the short length regime close to the origin. This is for just the same reason that the domain size distribution practically vanishes in the same region $y<l_c(t)$. Above the short length regime, $C_{pnnp}(y,t)$ increases rapidly and reaches a maximum value at $y \sim W(t)/2$. Above the peak, $C_{pnnp}(y,t)$ decreases rapidly and reaches a local minimum at $y \sim W(t)$. $C_{pnnp}(y,t)$ also shows oscillatory convergence to unity whose period of oscillation is also equal to $W(t)$. In addition, it should be mentioned that the functional forms of the number density correlation functions do not change along the entire coarsening process.

C. Dynamical scaling

Finally, a rescaling of the y and k_y axes by $W(t)$ is attempted. The scaled $g(l,t)$, $P_s(k_y,t)$, $C(y,t)$, $C_{ppnn}(y,t)$, and $C_{pnnp}(y,t)$ are shown in Figs. 15, 16, 17, 18, and 19, respectively. In each figure, the curves at different times fall on a universal curve. It is clearly shown experimentally that the dynamical scaling law holds in this coarsening process, as it is generally does for other space dimension systems [1–3,6].

IV. SUMMARY

Spinodal decomposition in a one-dimensional system with a conserved Ising order parameter was investigated experimentally utilizing the zigzag instability of walls in a nematic liquid crystal cell under magnetic and electric fields. It was found that the characteristic length increases logarithmically with time as had been expected from the theory [19] and the numerical simulation [20]. By the scaling analysis, it has been clarified that the dynamical scaling law holds in this coarsening process of a zigzag wall. The next stage of this research will be to undertake a comparison of the size distribution function of kinks among the experiments, theories, and numerical simulations. Until recently, no theoretical and numerical work had been undertaken to investigate the size distribution function of kinks. A detailed numerical simulation is now in progress by Toyoki [24]. The comparison of size distribution functions between the present experiment and the simulation will be reported shortly [24].

ACKNOWLEDGMENTS

We gratefully acknowledge Professor T. Kawakatsu, Professor H. Toyoki, and Professor H. Orihara for their constructive suggestions. This work was partly financed by the Centre National de la Recherche Scientifique of France.

[1] J. D. Gunton, M. San Miguel, and P. S. Sahni, *Phase Transitions and Critical Phenomena*, edited by C. Domb and J. L. Lebowitz (Academic, New York, 1983), Vol. 8, p. 267.

[2] A. J. Bray, Adv. Phys. **43**, 357 (1994); A. J. Bray, *Phase Transitions in Systems with Competing Energy Scales*, edited by T. Riste and D. Sherrington (Kluwer Academic, Boston, 1993); H. Toyoki, *Formation, Dynamics and Statistics of Patterns*, edited by K. Kawasaki, M Suzuki, and A. Onuki (World Scientific, Singapore, 1994), Vol. 2, p. 309.

[3] H. Orihara and Y. Ishibashi, J. Phys. Soc. Jpn. **55**, 2151 (1986).

[4] T. Ohta, D. Jasnow, and K. Kawasaki, Phys. Rev. Lett. **49**, 1223 (1982).

[5] T. Nagaya, H. Orihara, and Y. Ishibashi, J. Phys. Soc. Jpn. **56**, 1898 (1987); **56**, 3086 (1987); **59**, 377 (1990).

[6] T. Nagaya, H. Orihara, and Y. Ishibashi, J. Phys. Soc. Jpn. **60**, 1572 (1991); **61**, 3511 (1992); **64**, 78 (1995); H. Orihara, T. Nagaya, and Y. Ishibash, *Formation, Dynamics and Statistics of Patterns*, edited by K. Kawasaki, M Suzuki, and A. Onuki (World Scientific, Singapore, 1994), Vol 2, p. 157.

[7] A. Pargellis, N. Turok, and B. Yurke, Phys. Rev. Lett. **67**, 1570 (1991); A. N. Pargellis, J. Mendez, M. Srinivasarao, and B. Yurke, Phys. Rev. E **53**, R25 (1996).

[8] A. N. Pargellis, P. Finn, J. W. Goodby, P. Panizza, B. Yurke, and P. E. Cladis, Phys. Rev. A **46**, 7765 (1992).

[9] N. Mason, A. N. Pargellis, and B. Yurke, Phys. Rev. Lett. **70**, 190 (1993); B. Yurke, A. N. Pargellis, S. N. Majumdar, and C. Sire, Phys. Rev. E **56**, R40 (1997).

[10] I. Chuang, R. Durrer, N. Turok, and B. Yurke, Science **251**, 1336 (1991); I. Chuang, N. Turok, and B. Yurke, Phys. Rev. Lett. **66**, 2472 (1991); B. Yurke, A. N. Pargellis, I. Chung, and N. Turke, Physica B **178**, 56 (1992); I. Chuang, B. Yurke, A. N. Pargellis, and N. Turok, Phys. Rev. E **47**, 3343 (1993).

[11] K. Minoura, Y. Kimura, K. Ito, and R. Hayakawa, Mol. Cryst. Liq. Cryst. **302**, 345 (1997); K. Minoura, Y. Kimura, K. Ito, R. Hayakawa, and T. Miura, Phys. Rev. E **58**, 643 (1998).

[12] O. D. Laventovich and S. S. Rozhkov, Pis'ma Zh. Eksp. Teor. Fiz. **47**, 210 (1988); O. D. Lavrentovich and Y. A. Nastishin, Europhys. Lett. **12**, 135 (1990); O. D. Lavrentovich and Y. A. Nastishin, Kristallografiya **34**, 1529 (1989); O. D. Lavrentovich, Mol. Cryst. Liq. Cryst. **191**, 77 (1990); O. D. Lavrentovich and V. M. Pergamenshchik, *ibid.* **179**, 125 (1990); A. Sparavigna, L. Komitov, O. D. Lavrentovich, and A. Strigazzi, J. Phys. II **2**, 1881 (1992); O. D. Lavrentovich and V. M. Pergamenshchik, Phys. Rev. Lett. **73**, 979 (1994); O. D. Lavrentovich and V. M. Pergamenshchik, Int. J. Mod. Phys. B **9**, 2389 (1995).

[13] C. Chevallard, M. Clerc, P. Coullet, and J. M. Gilli, Eur. Phys. J. E. **1**, 179 (2000); C. Chevallard, M. Nobili, and J. M. Gilli, Liq. Cryst. **28**, 179 (2001).

[14] P. G. de Gennes and J. Prost, *The Physics of Liquid Crystals*, 2nd ed. (Oxford Science Publications, New York, 1993).

[15] J. W. Cahn and J. E. Hilliard, J. Chem. Phys. **28**, 258 (1958).

[16] T. Nagaya, J. M. Gilli, and C. Chevallard, in *Proceedings of the Conference 4ème Rencontres du Non linéaire 2001*, edited by I. Pomeau and R. Ribotta (Non Linéaire Publications, Orsay, 2001), p. 117.

[17] A. Vierheilig, C. Chevallard, and J. M. Gilli, Phys. Rev. E **55**, 7128 (1997); J. M. Gilli, M. Morabito, and T. Frisch, J. Phys. II **4**, 319 (1994); T. Frisch, Physica D **84**, 601 (1995); T. Frisch, S. Rica, P. Coullet, and J. M. Gilli, Phys. Rev. Lett. **72**, 1471 (1994).

[18] W. H. de Jeu, W. A. Claassen, and A. M. J. Spruijt, Mol. Cryst. Liq. Cryst. **37**, 269 (1976).

[19] A. D. Rutenberg and A. J. Bray, Phys. Rev. E **51**, 5499 (1995).

[20] T. Kawakatsu and T. Munakata, Prog. Theor. Phys. **74**, 11 (1985).

[21] T. Nagai and K. Kawasaki, Physica A **120**, 587 (1983); **134**, 483 (1986); K. Kawasaki and T. Nagai, *ibid.* **121**, 175 (1983); K. Kawasaki, A. Ogawa, and T. Nagai, Physica B **149**, 97 (1988).

[22] K. Kawasaki and T. Ohta, Physica A **166**, 573 (1982).

[23] M. Mondello and N. Goldenfeld, Phys. Rev. A **42**, 5865 (1990).

[24] H. Toyoki (private communication).